# Molecular Relaxation in Supersonic Free Jets of $N_2$ and $CH_4$ from Stimulated Raman Spectroscopy and Time-of-Flight Measurements

**L. Abad,[†] D. Bermejo,[‡] V. J. Herrero,*[,‡] J. Santos,[‡] and I. Tanarro[‡]**

*Departamento de Física Aplicada, Universidad Alfonso X el Sabio, Villanueva de la Cañada, 28601 Madrid, Spain, and Instituto de Estructura de la Materia (CSIC), Serrano 123, 28006 Madrid, Spain*

*Received: July 14, 1997*[⊗]

The relaxation of the energy stored in the translational and rotational degrees of freedom of $N_2$ and $CH_4$ in the course of free jet expansions has been experimentally studied. Rotational temperatures along the expansion axis were obtained by means of stimulated Raman spectroscopy, and terminal flow velocities and translational temperatures were determined from supersonic beam time-of-flight measurements. From these measurements low-temperature cross sections for rotational relaxation have been estimated. The results are compared with data from other experiments, and the validity of simple relaxation models is discussed.

## 1. Introduction

Free jets, characterized by the simultaneous occurrence of very fast cooling and rarefaction, provide a unique environment for the investigation of low-temperature processes in gases and offer many advantages for studies of spectroscopy, homogeneous nucleation, chemical reactivity, and collisional energy transfer.[1] In a typical free jet, formed in a supersonic expansion of a gas into a vacuum, most of the enthalpy in the gas source is transformed into kinetic energy of the flow, but the usually small amount of energy remaining as random translation or stored in the internal degrees of freedom contains very valuable information about the exchange of energy between the different molecular degrees of freedom (see refs 2−4 and references therein). In particular, free jets are very adequate for the study of momentum and rotational energy transfer, characterized by short relaxation times under ordinary circumstances. In this respect, the data from supersonic expansions complement and extend notably toward the low-temperature range other data from more conventional methods such as those based on viscosity or transport properties for the estimate of collision cross sections[5] or on ultrasonic and shock wave techniques for the investigation of rotational relaxation.[6]

The theoretical treatment of such a complex nonequilibrium system as a free jet poses formidable problems, which in general cannot be solved in a rigorous way.[7] In addition, detailed experimental determinations of the flow field with good spatial resolution are still exceptional.[8] Fortunately, the first part of a free jet expansion, characterized by a high collision frequency, is well described by the continuous isentropic model, which assumes local equilibrium (i.e. local macroscopic properties) and accounts for the transformation of the random internal energy of the gas into directed kinetic energy of the supersonic flow. Within this approximation, the properties of the jet flow field are determined everywhere by the Mach number, *Ma*, and the heat capacity ratio, $\gamma$, of the expanding gases. The Mach number, defined as the quotient between the flow velocity and the local speed of sound, is obtained from the numerical solution of the fluid mechanics equations. For the most common cases, useful analytical formulas have been fitted to these numerical results (see ref 4 and references therein). As collisions become less frequent, the gas molecules experience a gradual transition from continuous to free molecular flow and the local equilibrium among the different degrees of freedom of the system is no longer maintained. Ultimately collisions virtually cease and the flow properties, in particular the energy stored in the different degrees of freedom, remain frozen.

An accurate theoretical study of the transition from continuous to molecular flow in free jets would require the solution of a master equation of the Boltzmann type, taking into account the actual shape of the flow field and considering separately each individual internal state of the participating molecules. This is in general not possible and some approximations become unavoidable (see refs 4, 9, 10, and references therein). Free jet expansions from a circular nozzle are usually approximated as expansions of spherical symmetry, and the molecular velocities are separated into components parallel and perpendicular to the direction of a given streamline. In addition, instead of considering individual levels, it is often assumed that equilibrium is maintained within the distinct energy modes characterized by different temperatures. A common way of implementing this approximation consists of assuming a given form for the distribution function of molecular velocities and internal states depending parametrically on the flow velocity and the relevant temperatures. By generating the appropriate moments of the distribution, a set of differential equations coupling the evolution of the density, $n$, flow velocity, $u$, parallel and perpendicular translational temperatures, $T_{\|}$, $T_{\perp}$, and the different internal temperatures, $T_i$, can be obtained. A more simple treatment relating just the evolution of the temperatures, $T_{\|}$, $T_{\perp}$, $T_i$, during the expansion is provided by the "thermal conduction model".[11−13] Quite often the rotational degree of freedom is the only one to participate in the expansion, and $T_i$, reduces to $T_r$.

Even these simplified treatments are often difficult to apply due to lack of information about the simultaneous interrelation between the relevant magnitudes, and one must resort to further simplifications such as "sudden freeze" models, assuming a sharp stop in the evolution of a given property as the expansion proceeds,[11,14−16] or linear relaxation equations to describe the coupling between an individual energetic mode and the local thermal bath provided by the jet.[16−19] These simple models are the most widely used in the design and analysis of experiments involving free jets and supersonic molecular beams; however, the physical approximations implied in them are too

* Corresponding author.
[†] Universidad Alfonso X el Sabio.
[‡] Instituto de Estructura de la Materia.
[⊗] Abstract published in *Advance ACS Abstracts,* November 15, 1997.

S1089-5639(97)02277-9 CCC: $14.00 

extreme and not easily justifiable and the range of validity of these simple models should be experimentally assessed.

In the present work we have investigated the translational and rotational relaxation in supersonic free jets of two small molecules, $N_2$ and $CH_4$, with different values of the heat capacity ratio, giving thus rise to different supersonic flow fields. Since both molecules have a relatively small tendency to form aggregates, a wide range of expansion conditions can be sampled for relaxation studies. In addition, experimental relaxation data from other techniques are available in the literature, especially for nitrogen, and can be used as a reference.

Attempts to measure local translational temperatures in free jets of $N_2$ from Doppler broadening of spectral lines were unsuccessful,[20] and the available information about translational relaxation comes from time-of-flight (TOF) measurements performed on the supersonic molecular beams obtained by skimming the central part of the jet.[17,21,22] Time-of-flight measurements are also available for supersonic beams of methane.[18,21]

A wide variety of experimental techniques have been applied for the determination of rotational temperatures in free jets of $N_2$; these techniques include energy balance in conjunction with time-of-flight measurements,[17,18,23] spontaneous Raman scattering,[24] coherent anti-Stokes Raman spectroscopy (CARS),[25,26] electron beam induced fluorescence,[22,27−31] and resonance-enhanced multiphoton spectroscopy (REMPI).[32] Rotational temperatures of methane in free jets have been obtained from spontaneous Raman scattering,[24] CARS,[33] stimulated Raman spectroscopy (SRS),[34] and Fourier transform infrared (FTIR) spectroscopy.[35]

Some of the above-mentioned experimental measurements are too indirect (energy balance) and do not provide a distribution of internal states. In some other techniques, especially in those involving transitions to electronic states, the derivation of the populations of internal states from the experimental data is not straightforward and controversies about the interpretation of the results have appeared (see discussion in ref 36). IR, Raman, and SRS are more direct techniques for the determination of internal states populations, but their sensitivity is low.

In general, relaxation studies in supersonic expansions are based on data restricted either to the first part of the free jet (i.e. to the vicinity of the nozzle) or to terminal properties measured in the collision free region after the end of the expansion, but as a rule, no simultaneous data for both regions are reported in the same experiment. On the other hand, some of the above-mentioned experimental measurements were mainly intended as demonstrations of new spectroscopic techniques or as a practical means of simplifying congested spectra rather than to the systematic investigation of free jet properties or relaxation phenomena.

In our experiments, we combine experimental data (rotational-state populations) from SRS spectra close to the nozzle exit with information about the end of the expansion (final translational hydrodynamic velocity and parallel translational temperatures obtained from time-of-flight measurements). The results are analyzed in terms of simple relaxation models and compared to experimental data obtained with other techniques.

## 2. Experimental Section

The experimental setup used in the present work is described elsewhere,[37−39] and only the most relevant details will be given here. Nitrogen and methane were expanded from a commercial solenoid driven pulsed valve. The source pressures, $p_0$, ranged from 190 to 3500 mbar for $N_2$ and from 260 to 5000 mbar for $CH_4$. In all the experiments the pulsed valve was kept at room temperature ($T_0 = 296$ K). The jet source was mounted on a movable base that could be displaced under vacuum. The movement along the beam axis was achieved by means of a linear motion feedthrough provided with a micrometric screw. Nearly square gas pulses of about 1 ms duration were used in the present experiments. Both the TOF and SRS measurements were performed on the central part of the gas pulses (quasi steady state), and special care was paid to the determination of the effective nozzle diameter, $d_{\text{eff}}$, from measurements of the gas flow to the expansion chamber.[37] The $d_{\text{eff}}$ values were found to be 20−30% smaller than the nominal diameter of 0.5 mm. The gas pulses were expanded into a 50 L chamber pumped by a 2000 L $s^{-1}$ oil diffusion pump.

For the TOF measurements, the expansion chamber was connected with the detection system through a conical 0.8 mm diameter skimmer. The detection system consisted of three interconnected vacuum chambers: the first contained a mechanical chopper, the second provided for differential pumping, and the third one contained the quadruopole mass spectrometer used as a detector. The nozzle skimmer distance was usually 8−10 cm, and the pulse frequency of the valve was made slow enough as to keep the average background pressure in the $10^{-5}$ mbar range in order to avoid attenuation of the beam; beyond the skimmer the pressure was lower than $5 \times 10^{-6}$ mbar. The flight path between chopper and detector was ≈60 cm, and the geometric gate function of the chopper was a Gaussian with a fwhm of 23 $\mu$s. The pressure in the detector chamber was always in the $10^{-7}$ mbar range.

For the SRS measurements pump and probe laser beams with parallel polarization were focused on the axis of the expanding jet inside the vacuum chamber. The probe beam was provided by a stabilized $Ar^+$ laser operating in single mode at 514 nm. The output signal had a bandwidth of less than 1 Mhz and a power of about 350 mW. For the pump beam, the emission of a ring dye laser operated with Rhodamine 6G was pulse amplified in a three stage amplifier, pumped by the second harmonic of a seeded Nd:YAG laser with an extended cavity. Sulforodamine 640 and Kiton red were used in the amplifier for the $CH_4$ and $N_2$, respectively. The output of the pump laser consisted of 12 ns pulses with a temporal and spatial Gaussian shape and with a bandwidth of ≈100 Mhz limited by the Fourier transform of the time width of the pulses. The energy per pulse was about 7 mJ and the repetition rate 14 Hz. Laser and valve pulses were synchronized by means of a pulse generator. The spectroscopic signal, given by the intensity loss of the probe laser beam, was detected with a fast photodiode and acquired by means of a boxcar averager.

The spectra were recorded in the region between 2329 and 2330 $cm^{-1}$ (fundamental vibrational mode) for $N_2$ and in the region between 2916.40 and 2917.95 $cm^{-1}$ for $CH_4$, which corresponds to the $\nu_1$ stretching fundamental. Figure 1 shows a global scheme of the supersonic expansion and of the kind of information obtained from the experimental measurements.

## 3. Results and Analysis

The velocity distributions of the molecules at the end of the supersonic expansion (terminal distributions) are obtained from the time-of-flight measurements. Due to the favorable experimental conditions made possible by the pulsed beam arrangement (low background pressure and large nozzle skimmer distances), beam gas interaction and skimmer interference are expected to be negligible and the measured distributions should reflect the actual terminal properties. For the analysis of the TOF spectra, we have considered that at large distances from the nozzle exit the expansion has an approximately spherical

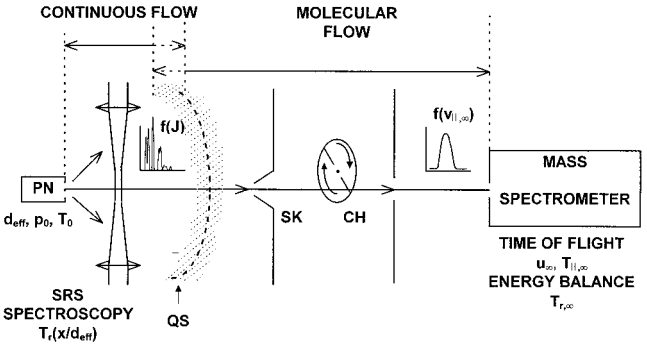


**Figure 1.** Scheme of the experimental setup with indication of the type of information obtained from the stimulated Raman spectroscopy (SRS) and time-of-flight (TOF) measurements. The meaning of the symbols is as follows: PN, pulsed nozzle; $p_0$, $T_0$, pressure and temperature of the gas source; $d_{\text{eff}}$, effective nozzle diameter; QS, quitting surface; SK, skimmer; CH, chopper; $T_r(x/d_{\text{eff}})$, rotational temperature as a function of the distance to the nozzle; $f(J)$ distribution of rotational states; $f(v_{||,\infty})$ terminal distribution of parallel velocities; $u_\infty$, terminal flow velocity; $T_{||,\infty}$, terminal parallel temperature; $T_{r,\infty}$ terminal rotational temperature.

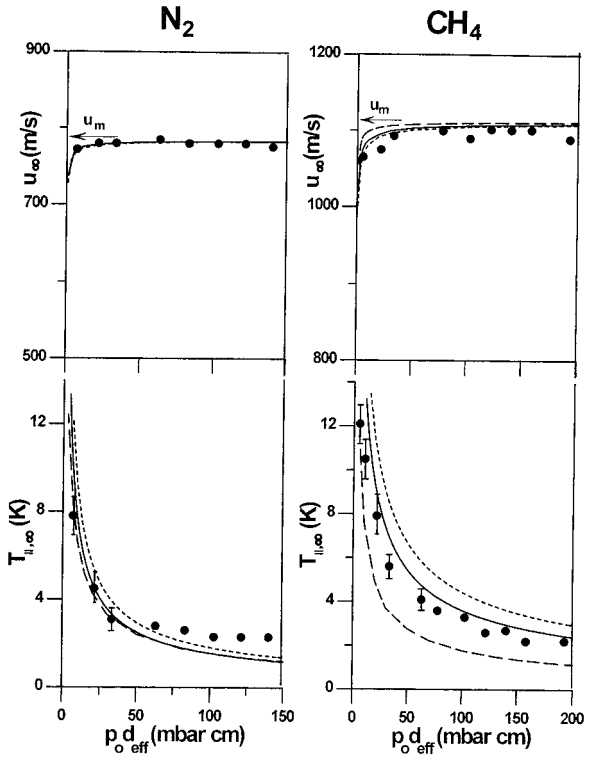


**Figure 2.** Terminal flow velocities, $u_\infty$, and parallel temperatures, $T_{||,\infty}$, in supersonic free jets of nitrogen and methane as a function of the product of source pressure and effective nozzle diameter, $p_0 d_{\text{eff}}$. The full circles are the experimental measurements, the solid lines are results of the sudden freeze model of eq 4 (refs 4,11) with the temperature dependent collision cross section given by eq 5, the short dashed line represents the results of the same model with a temperature independent rigid sphere collision cross section, and the long dashed line corresponds to the semiempirical correlation of Brusdeylins and Mayer.[21] The arrows labeled $u_m$ indicate the maximum flow velocity allowed by conservation of energy.

symmetry and the molecular velocities can be separated into components parallel, $v_{||}$, and perpendicular, $v_\perp$, to a given streamline. Our measurements, performed on a collimated supersonic beam, sample essentially the distribution of velocities parallel to the axial streamline. This distribution is assumed to be of the usual "drifting Maxwellian" type,[4,40] i.e., a Maxwellian distribution characterized by a temperature $T_{||}$, traveling with the flow velocity $u$. The terminal values of the flow velocity $u_\infty$ and parallel temperature, $T_{||,\infty}$, or speed ratio, $S_{||,\infty} = (mu_\infty^2/2kT_{||,\infty})^{1/2}$, where $m$ is the molecular mass and $k$ the Boltzmann constant, are obtained by a standard deconvolution of the time-of-flight data.[41,42] The results are represented in Figure 2 as a function of the product $p_0 d_{\text{eff}}$, which, for a given source temperature, is inversely proportional to the source Knudsen number. Even for the weakest expansions studied, the terminal flow velocities are more than 95% of the maximum value allowed by the conservation of energy, $u_m = [2\gamma kT_0/(\gamma - 1)m]^{1/2}$, indicating a very efficient conversion of internal energy of the gas into kinetic energy of the flow; consequently, translational relaxation is nearly complete and the final translational temperatures are very low. For $p_0 d_{\text{eff}}$ values larger than 50 mbar cm, the $T_{||,\infty}$ for both molecules are in the 2−4 K range.

The rotational temperatures along the jet axis were obtained by simulating the SRS spectra. Distorted shapes of the SRS lines were observed in the region immediately downstream of the nozzle exit. These distortions can be attributed to collisional broadening in a region where the pressure is still high (especially in the strongest expansions) and to the strong gradients of density and temperature occurring in the direction perpendicular to the jet axis in the first nozzle diameters.[43] A model[44] taking into account the detailed distributions of density, temperature, and perpendicular flow velocities can reproduce the observed line shapes. Beyond ≈4−5 nozzle diameters, which is the region of main interest to the present work, collisional broadening disappears, the thermal Doppler widths become very small, due to the strong cooling of the expansion, and the model shows that the line widths are essentially determined by the distribution of transversal components of the flow velocity associated with the angular divergence of the jet. The spectral lines in this region can be approximated by Gaussian functions, whose width must be slightly adjusted for each experimental spectrum. For the simulation of the SRS spectra we have made the usual assumption that the different nuclear spin modifications of a given species do not interconvert in the course of the expansion due to the very low rate of the nuclear spin relaxation, and we have thus considered the room-temperature abundance ratios of the various nuclear spin varieties for the simulation of all the jet spectra. Within this assumption the spectra could always be satisfactorily reproduced by using Boltzmann distributions with the same temperature for all the spin varieties. Illustrative examples of the measured spectra together with their theoretical simulations are shown in Figures 3 and 4. In Figure 3 we have represented two spectra of nitrogen taken at the same distance from the nozzle exit and corresponding to two different expansions. As can be seen, the rotational temperature is lower by about 6 K for the stronger expansion. Figure 4 shows an analogous effect for $CH_4$, but in this case the distance to the nozzle exit is larger and the temperature difference is somewhat higher (≈10 K). For both substances, the spectra represented in the left part of Figures 3 and 4 correspond to the low $T_r$ range for the weakest expansions studied, where a departure from equilibrium between the different rotational states would be most likely to occur; but the spectra can be satisfactorily simulated within experimental error. The rotational temperatures obtained for $N_2$ and $CH_4$ along the expansion axis are represented in Figures 5 and 6 together with measurements by other authors using different experimental techniques.

The mass spectroscopic analysis of our supersonic beams showed that in our room-temperature expansions the fraction of dimer-ion to monomer-ion reached an approximate value of 0.5% for expansions of nitrogen with $p_0 d_{\text{eff}} \approx 150$ mbar cm

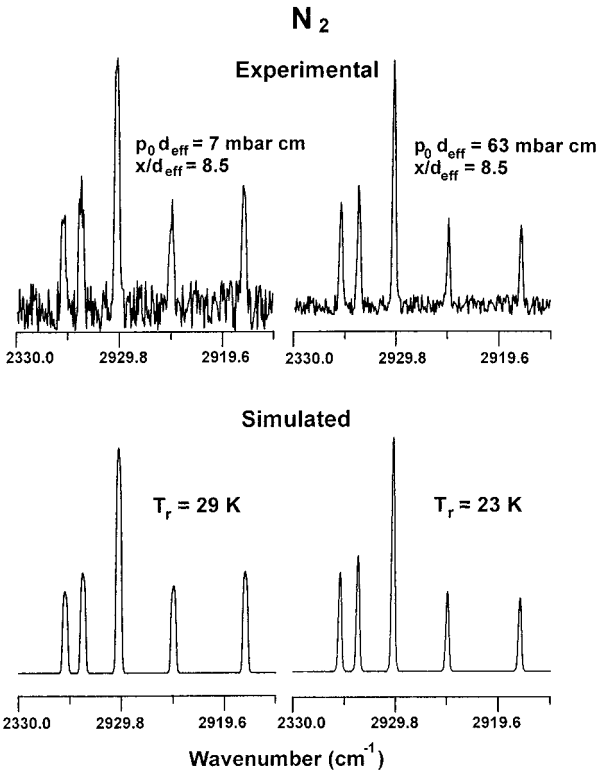


**Figure 3.** Experimental and simulated SRS spectra taken in free jets nitrogen at the same distance from the nozzle exit for different expansion conditions. Lines from $j = 0$ to $j = 5$ are shown.

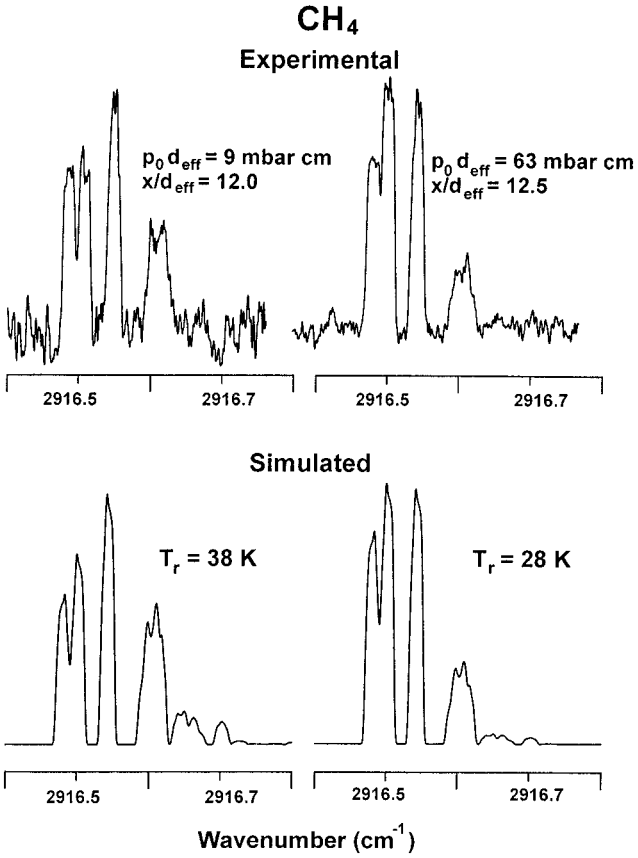


**Figure 4.** Same as Figure 2, but for free jets of methane. For the assignment of spectral lines see ref 39.

and for expansions of methane with $p_0 d_{\text{eff}} \approx 200$ mbar cm. We have restricted the present study to expansions with $p_0 d_{\text{eff}}$ lower than these values in order to ensure that aggregation processes are insignificant. On the other hand, the fundamental vibrational

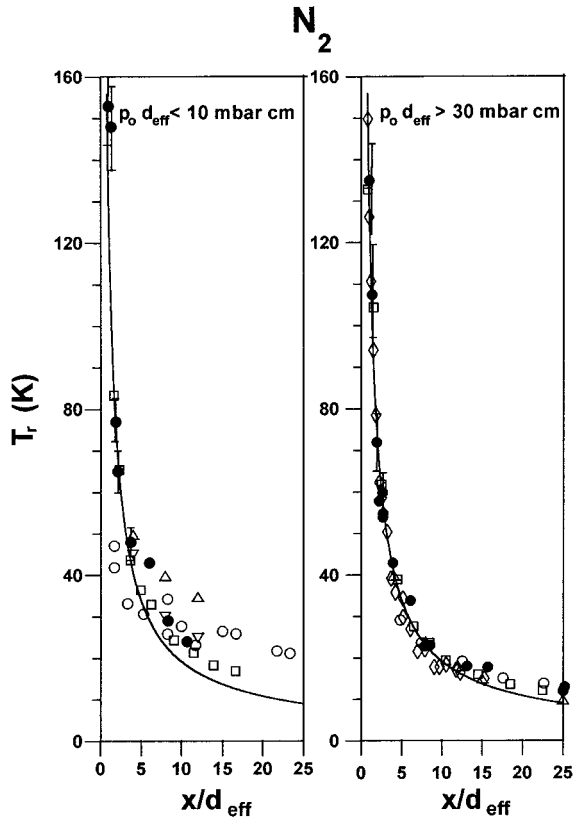


**Figure 5.** Rotational temperatures measured by different experimental techniques in free jets of nitrogen from room-temperature sources corresponding to different expansion conditions. Left panel: weaker expansions. Full circles present SRS results for $p_0 d_{\text{eff}} = 7$ mbar cm; open circles, REMPI measurements from ref 32 for $p_0 d_{\text{eff}} = 9$ mbar cm; open squares, CARS measurements from ref 26 for $p_0 d_{\text{eff}} = 7.5$ mbar cm; triangles, electron beam fluorescence measurements from ref 29 for $p_0 d_{\text{eff}} = 2.1$ mbar cm; inverted triangles, measurements from the same reference with $p_0 d_{\text{eff}} = 4.2$ mbar cm. Right panel: strong expansions. Solid circles present results for $p_0 d_{\text{eff}} = 63$ mbar cm; open squares, Raman measurements from ref 24 for $p_0 d_{\text{eff}} = 33$ mbar cm; open circles, CSRS measurements of ref 54 for $p_0 d_{\text{eff}} = 40$ mbar cm; open diamonds, CARS measurements of ref 26 for $p_0 d_{\text{eff}} = 103$ mbar cm; open triangles, electron beam fluorescence measurements of ref 29 for 34 mbar cm. The solid line corresponds to the $\gamma = 7/5$ isentropic curve.

frequency of $N_2$ is 2331 $cm^{-1}$, and that of the lowest mode of $CH_4$ is 1306 $cm^{-1}$. At room temperature the amount of molecules in excited vibrational states is thus negligible, and in addition the number of collisions required to relax these modes is very high;[6] consequently, for the conditions of the present experiments, the vibrational modes are not expected to participate in the expansion. Under the assumptions of equilibrium along a streamline, no clustering and no vibrational relaxation, the approximate terminal rotational temperature of the molecules can be estimated from an energy balance. Following the axial streamline, one can express the conservation of source enthalpy at the position of the mass spectrometer detector as[22,40]

$$\left(\frac{5}{2}k + C_r\right)T_0 = \frac{3}{2}kT_{\parallel,\infty} + C_r T_{r,\infty} + \frac{1}{2}mu_\infty^2 \qquad (1)$$

where $C_r$ is the rotational contribution to the specific heat capacity. In the balance expressed by eq 1 it has been taken into account that the perpendicular temperature, $T_\perp$, tends to zero for very long distances from the nozzle exit. By assuming a constant heat capacity ratio, $\gamma = 7/5$ for $N_2$ and $\gamma = 8/6$ for $CH_4$, the terminal rotational temperatures can be written as

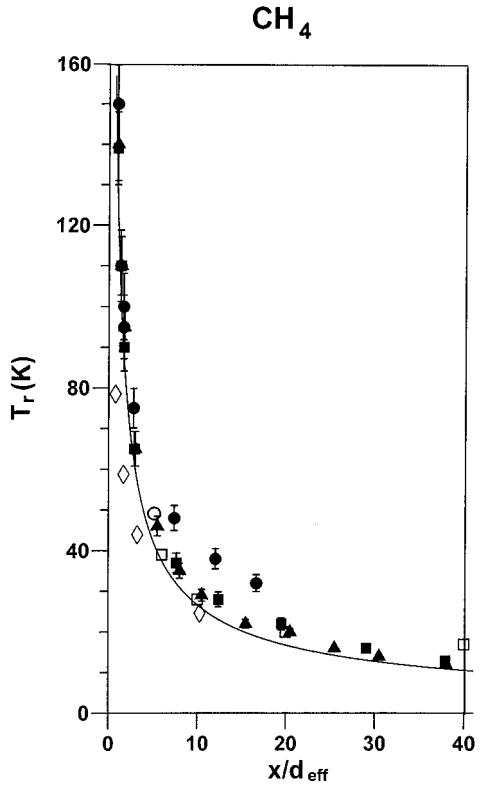


**Figure 6.** Same as Figure 5, but for $CH_4$ free jets. Solid symbols present SRS measurements; circles, $p_0d_{\text{eff}} = 9$ mbar cm; squares, $p_0d_{\text{eff}} = 63$ mbar cm; triangles, $p_0d_{\text{eff}} = 140$ mbar cm; open circle, SRS measurement from ref 34 for $p_0d_{\text{eff}} = 12$ mbar cm; open squares, Raman measurements from ref 24 for $p_0d_{\text{eff}} = 175$ mbar cm; open diamonds, CARS measurements from ref 33 for $p_0d_{\text{eff}} = 150$ mbar cm. The solid line corresponds to the $\gamma = 8/6$ isentropic curve.

$$T_{r,\infty}(N_2) = \frac{7}{2}T_0 - \frac{3}{2}T_{||,\infty} - \frac{mu_\infty^2}{2k} \quad (2)$$

$$T_{r,\infty}(CH_4) = \frac{8}{3}T_0 - T_{||,\infty} - \frac{mu_\infty^2}{3k} \quad (3)$$

Once $u_\infty$ and $T_{||,\infty}$ are known from the TOF measurements, the derivation of the terminal rotational temperature is straightforward. However, under our experimental conditions, the imprecision in the values of $T_{r,\infty}$ is large, as shown in Figures 7 and 8, due to the fact that most of the energy of the jet is carried by the $mu_\infty^2$ term. A 1% error in the value of the final flow velocity leads to an uncertainty of 5−15 K in $T_{r,\infty}$.

## 4. Discussion

Although in some cases, master equations including state specific relaxation rate constants have indeed been used for the study of rotational relaxation in jets,[23,45−47] in general, neither the quality of the experimental data nor the current knowledge of the mentioned rate constants or of the precise flow field shape warrant conclusions about the relaxation of individual rotational states. The solution of the Boltzmann equation by the method of moments and the thermal conduction model, mentioned in the Introduction, provide interesting insights into the relaxation processes taking place in free jets and in particular account in a natural way for the anisotropy in translational cooling and for the breakdown of equilibrium between the various energetic modes in the expansion. Both approaches have been used for the study of expansions of monatomic gases,[9,11] binary mixtures,[48] and small molecules,[10,13] but in general, the available

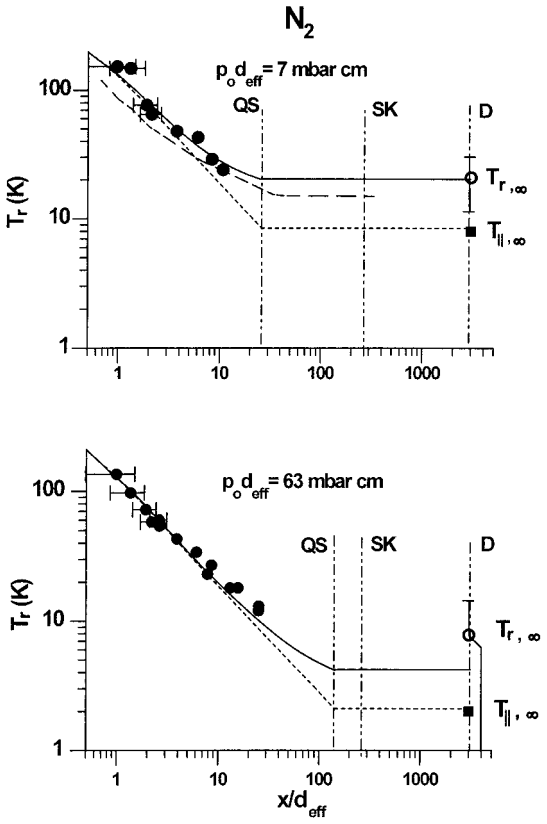


**Figure 7.** Evolution of temperatures in free jets of nitrogen: full circles, rotational temperatures from SRS measurements; closed squares, terminal translational temperatures from time-of-flight measurements; open circles, terminal rotational temperatures from energy balance; solid line, rotational temperature given by eq 6 using the cross section expression of eq 8 with $\sigma_{r,0} = 10$ Å$^2$ and $c = 0.6$; short dash line, isentropic curve for $\gamma = 7/5$; long dash line (upper panel), results of the Boltzmann equation model reported in ref 10 for $p_0d_{\text{eff}} = 12$ mbar cm. QS, SK, and D indicate the locations of the quitting surface, skimmer, and detector, respectively.

information about the coupling between the relevant magnitudes is insufficient, and further simplifying assumptions must be made in order to apply these treatments to practical cases.

Due to the difficulties for the application of the above-mentioned treatments, especially in the investigation of molecular free jets, we have resorted to more drastic approximations such as the "sudden freeze" model for the derivation of terminal properties and a linear relaxation equation for the description of the coupling of the rotational motion to the translational bath throughout the expansion.

The sudden freeze model for the translational motion[11,14] assumes that the expansion is continuous (i.e. describable in terms of local macroscopic variables) up to a given distance where collisions cease abruptly. Beyond this distance ("quitting surface") the flow is molecular. In the region of continuous flow the translational motion behaves isentropically and $T_{||} = T_\perp = T$. The quitting surface is assumed to be located at a point where the number of remaining two-body collisions is close to unity. Current expressions for the terminal speed ratios or temperatures can be found in the literature.[4,11,22] In Figure 2, we compare our experimental data to the theoretical model of Beijerinck and Verster,[4,11] which relates the final speed ratio to the source Knudsen number, $Kn_0$, by a functionality of the type:

$$S_{||,\infty} = A(Kn_0^{-1})^B \quad (4)$$

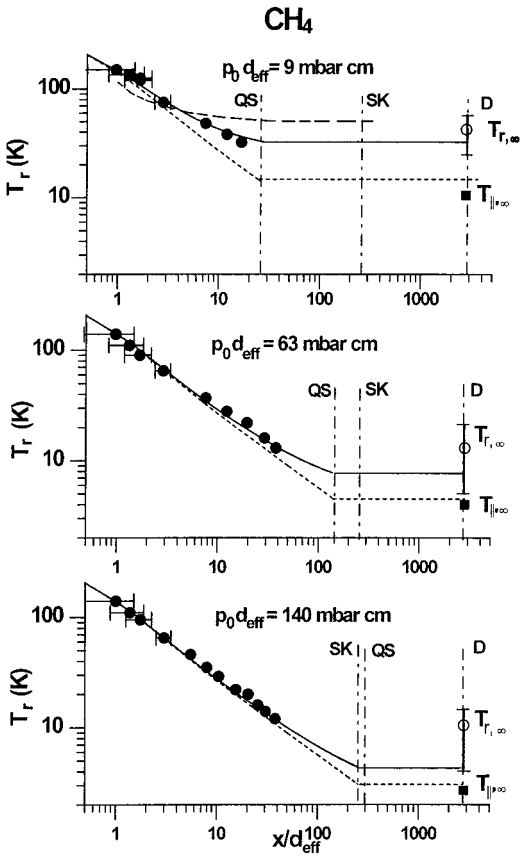


**Figure 8.** Evolution of temperatures in free jets of methane: solid line, rotational temperature from eq 6 using the cross section expression of eq 8 with $\sigma_{r,0} = 5$ Å$^2$ and $c = 0.9$; short dash line, isentropic curve for $\gamma = 8/6$; long dash line (upper panel), results of the Boltzmann equation model reported in ref 10 for $p_0 d_{eff}$ =12 mbar cm. The rest of the symbols are the same as in Figure 7.

where $A$ and $B$ are constants depending on $\gamma$. In the derivation of eq 4 a viscosity-based collision cross section determined by the attractive part of the intermolecular potential was assumed. This cross section can be approximately expressed as[4]

$$\sigma_c \approx (53C_6/kT)^{1/3} \tag{5}$$

where $C_6$ corresponds to the attractive term of a Lennard-Jones (L-J) potential. The assumption of a collision cross section based on the attractive part of a L-J potential has proven adequate for the description of collisional processes in supersonic expansions of monatomic gases[3,9,11] with the exception of He at very low temperatures,[9] where quantum effects can lead to an increase in $\sigma_c$ significantly more pronounced than the $T^{-1/3}$ dependence of eq 5. For collisions at high temperatures, a hard sphere cross section should be more adequate than a $\sigma_c$ based on attractive forces.

For the comparison of the terminal properties predicted by the model of eq 4 with our experimental data, we have taken[5] $(C_6/k) = 9.2 \times 10^{-43}$ K cm$^{-6}$ and $18 \times 10^{-43}$ K cm$^{-6}$ for $N_2$ and $CH_4$, respectively, and the parameters used in eq 4 are $A = 0.783$ and $B = 0.353$ for $N_2$ ($\gamma = 7/5$) and $A = 0.920$ and $B = 0.297$ for $CH_4$ ($\gamma = 8/6$). As a reference, we have also calculated terminal properties from eq 4 with a temperature independent hard sphere cross section $\sigma_c = \pi r^2$, where $r$ has been identified with the length parameter of the L-J potential ($r = 3.7$ Å for $N_2$ and 3.81 Å for $CH_4$).

The experimental information about terminal properties in molecular expansions[21,22] is more limited than that for expansions of monatomic gases. Brusdeylins and Mayer[21] have provided a semiempirical correlation obtained from a fit to their time-of-flight measurements on supersonic molecular beams of diatomic and small polyatomic molecules (including $N_2$ and $CH_4$). In their experiments, the molecular beams were generated from room-temperature sources with $p_0 d_{eff} < 100$ mbar cm. The terminal temperatures and flow velocities corresponding to this correlation are also represented in Figure 2.

The sudden freeze model of eq 4 using the cross section expression of eq 5 can approximate the present experimental values of the terminal translational temperatures of $N_2$ and $CH_4$ within $\approx$1 K and gives the best global agreement with experiment. In the case of nitrogen, the use of a hard sphere cross section or the semiempirical correlation of Brusdeylins and Mayer leads to very similar results. For methane, the differences between the three curves are larger, but in any case, they can reproduce most experimental points within 2 K. It is interesting to observe that the model of eq 4 can reproduce the slower terminal cooling as a function of $p_0 d_{eff}$ obtained for methane as compared with $N_2$. This is due to the lower $\gamma$ of methane that leads to a more gradual transformation of internal energy into directed energy of the flow. As a consequence, stronger expansions, shifting the quitting surface further from the nozzle exit, are needed in order to achieve the same degree of cooling. This is illustrated in Figures 7 and 8. For $p_0 d_{eff}$ values larger than $\approx$140 mbar cm, the quitting surface calculated from the model is located beyond the skimmer, and under these circumstances the terminal properties could be determined by the diaphragm; however, this is already a jet region of very low density and slow varying properties and no significant changes are observed neither in the measurements nor in the model predictions. The terminal temperatures obtained with the rigid sphere cross section are slightly higher, as expected, than those from the $\sigma_c$ based on the attractive part of the potential, but the differences are small, reflecting the fact that at room temperature and slightly below, where the majority of collisions determining the translational cooling take place, the rigid sphere assumption is a good approximation to the collision cross section. However, the $T^{-1/3}$ temperature dependence of the collision cross section is important for processes taking place at very low temperature like the breakdown of equilibrium between rotation and translation discussed below.

The location of the quitting surface determines also the terminal flow velocity, $u_\infty$. The final velocities predicted by the model for our expansions ($p_0 d_{eff} > 5.4$ mbar cm) are always within 5% of the maximum flow velocity compatible with the conservation of energy, $u_m$, in agreement with our experimental measurements. The terminal flow velocities measured for methane are smaller by about 1% than the predictions of the models and, in the region below 50 mbar cm, reflect also the slower transfer of random energy to kinetic energy of the flow associated with the lower $\gamma$ of methane.

The linear relaxation equation coupling rotational temperature to the thermal bath provided by the jet can be expressed as[16−19]

$$\frac{dT_r}{dt} = -\frac{1}{\tau_r}(T_r - T) \tag{6}$$

where $\tau_r$ is a characteristic rotational relaxation time. This expression is analogous to the one used for the study of bulk equilibration processes and is also obtained as an approximation in the more elaborate treatments of supersonic expansions commented on above.[10,12] For small deviations of $T_r$ from equilibrium, an approximate isentropic behavior can be assumed for the jet with $T_\parallel \approx T_\perp \approx T$, and the isentropic relations can be used to express the time evolution of $T_r$ as a function of the

Mach number and the heat capacity ratio. The rotational relaxation time can be interpreted as the inverse of a collision frequency for rotational relaxation and can thus be related to the corresponding rotational relaxation cross section, $\sigma_r$, through $(\tau_r)^{-1} = 4n(kT/\pi m)^{1/2}\sigma_r$, where $n$ is the number density of molecules. If the sudden freeze model of the previous paragraph is assumed, the terminal rotational temperature, $T_{r,\infty}$, is given by the solution of eq 6 at the quitting surface.

The cross section for rotational relaxation is often related to the collision cross section, $\sigma_c$, by means of the rotational collision number, $z_r$, which can be expressed as[17,18]

$$z_r = \sigma_c/\sigma_r \tag{7}$$

This parameter is widely used for the characterization of rotational relaxation experiments of different kinds.[6] In the literature, there is some ambiguity about the cross sections used for the definition of $z_r$, and care should be taken in the comparison of data from different sources. In some jet experiments a single effective $z_r$ is used for the description of the whole expansion,[18,22,24,29] but given the large temperature variation throughout a free jet, this assumption of a single $z_r$ is not justified a priori. By taking into account that the departure of rotation from equilibrium will take place close to the end of the expansion, realistic estimates of the low-temperature $z_r$ should be obtained if one uses the $\sigma_c$ value corresponding approximately to $T_\infty$;[19] this procedure could lead to different $z_r$ for weak and strong expansions of the same gas. In other experiments a rigid sphere collision cross section is used and a temperature-dependent $z_r$ is obtained;[17,25,49] in this case, the temperature dependences of both $\sigma_r$ and $\sigma_c$ are mixed in the temperature evolution of the rotational collision number. In other experimental studies[26,30,31] and in most theoretical works,[10,12,50] a distinct temperature dependence is considered for both $\sigma_c$ and $\sigma_r$.

In our study we have assumed for $\sigma_r$ a simple temperature dependence of the form

$$\sigma_r = \sigma_{r,0}(T_0/T)^c \tag{8}$$

where $\sigma_{r,0}$ is the room-temperature rotational relaxation cross section. The parameters $\sigma_{r,0}$ and $c$ have been obtained by simulating with eq 6 the measured evolution of the rotational temperatures along the jet axis. Only one pair of parameters has been used to fit all the data corresponding to a given gas. For the derivation of these parameters we have taken into account that the experiments of the present work, and in general, experiments carried out in supersonic jets from room-temperature sources are not sensitive to the value of $\sigma_r$ in the higher temperature region close to the nozzle exit, where two-body collisions are still frequent. Consequently, the $\sigma_{r,0}$ parameter has been maintained within the range of most bibliographic data which are mainly from acoustic techniques (see refs 6, 17, 49 and references therein). The values finally obtained were $\sigma_{r,0} = 10$ Å,$^2$ $c = 0.6$ for $N_2$ and $\sigma_{r,0} = 5$ Å,$^2$ $c = 0.9$ for $CH_4$. Belikov et al.[30,31] have determined rotational relaxation cross sections for nitrogen over the 6−320 K temperature range and indicate that the $c$ exponent of eq 8 is in fact temperature dependent. However our experiments are only sensitive to temperatures between approximately 15 and 100 K. For this temperature range and for the precision of our data, the functionality given in eq 8 seems to be adequate. In Figure 9 we have represented the evolution of the rotational relaxation cross sections for nitrogen and methane obtained from our data together with other experimental and theoretical estimates (see below). Over the 15−100 K range, our $\sigma_r$ values correspond

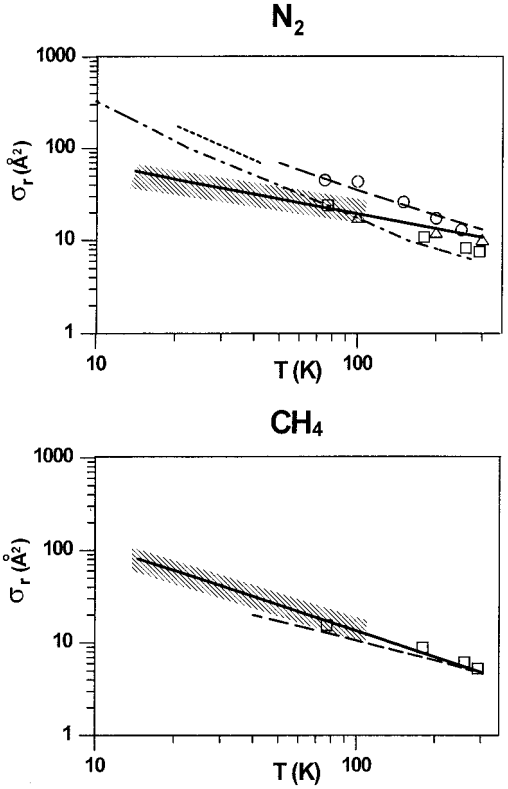


**Figure 9.** Rotational relaxation cross sections for $N_2$ and $CH_4$. Upper panel: cross sections for nitrogen. Solid line, present results; open squares, ultrasonic measurements from ref 49; open circles, TOF and energy balance from ref 17; open triangles, trajectory calculations from ref 51; dash−dot line, electron beam fluorescence from ref 31; long dash line, Monte Carlo calculations from ref 50; short dash line, CARS measurements of ref 26. Lower panel: cross sections for methane. Symbols are the same as in upper panel. The hatched areas indicate the approximate range of relaxation cross sections compatible with our measurements.

to rotational collision numbers ranging approximately from 2 to 3.5 for nitrogen and 2 to 6.5 for methane. The hatched areas represent the range of relaxation cross sections compatible with our measurements.

The results of the application to our experimental data of the simple translational and rotational relaxation models just commented on are summarized in Figures 7 and 8. In these figures we have represented, together with the measured temperatures, the isentropic curve, the evolution of rotational temperature calculated with the linear relaxation equation, and the positions of the quitting surface, skimmer, and the (mass spectrometer) detector with respect to the nozzle exit. In the two weakest expansions ($p_0 d_{eff} = 7$ mbar cm for $N_2$ and $p_0 d_{eff} = 9$ mbar cm for $CH_4$), the measured $T_r(x/d_{eff})$ deviate from the isentropic behavior with increasing distance to the nozzle exit. For the stronger expansions the separation of the observed $T_r(x/d_{eff})$ from the isentropic curve is much smaller and happens at larger distances. As can be seen, eq 6 with the $\sigma_{r,0}$ and $c$ parameters given in the previous paragraph can account reasonably well for the measured $T_r(x/d_{eff})$ in all cases, and the final rotational temperatures obtained from this equation at the quitting surface are always within the (large) error bars of the $T_{r,\infty}$ determined from the energy balance expressed in eqs 2 and 3. The measured values of $T_{ll,\infty}$ correspond approximately to the isentropic temperatures at the quitting surface as indicated in the discussion of Figure 2, and that lends support to the assumption of nearly isentropic behavior of the translational motion close to the end of the expansion, i.e., in the region relevant for the breakdown of equilibrium between translation

and rotation. Randeniya and Smith[10] have applied a model based on the approximate solution of the generalized Boltzmann equation for the prediction of rotational and translational temperatures in relatively weak ($p_0d_{eff}$ = 12 mbar cm) expansions of nitrogen and methane. For the expansion of nitrogen, they also report calculations performed with the thermal conduction model of Klots.[12] The expression of the characteristic relaxation time, $\tau_r$, is slightly different in each of these models, but both use a temperature independent parameter (also different in each model), taken from a fit to diverse literature data, to account for the fraction of relaxing collisions. In the upper panels of Figures 7 and 8 we have represented the $T_r(x/d)$ reported by Randeniya and Smith from their model based on the solution of the generalized Boltzmann equation; although the authors also provide $T_{||}$ and $T_{\perp}$, we have only represented the evolution of the rotational temperatures that can be compared directly to our measurements. The asymptotic temperatures obtained for the expansion of nitrogen with both models ($T_{r,\infty} \approx 15$ K; $T_{||,\infty} = 8-9$ K) do not differ much from the values of our nitrogen jet with $p_0d_{eff}$ = 7 mbar cm (see upper panel of Figure 7). For $CH_4$ the $T_r$ predicted by the model based on the generalized Boltzmann equation beyond 8−10 nozzle diameters are higher than those observed in our experiment with $p_0d_{eff}$ = 9 mbar cm. For both molecules, the results of this model seem to underestimate the experimental $T_r$ for distances of a few nozzle diameters, but given the uncertainty in the knowledge of the actual origin of the expansion, one should be cautious with the comparisons in this region.

The rotational relaxation cross sections, $\sigma_r(T)$, obtained from the present measurements within the linear relaxation model of eqs 6−8, are represented in Figure 9 together with the results from other measurements and calculations. For this comparison we have used only references in which a temperature dependence for $\sigma_r$ is reported. Data presented in the literature in the form of rotational collision numbers were transformed into cross sections via eq 7.

The rotational relaxation of $N_2$ has been extensively investigated over a wide temperature range. We will limit the present discussion to data corresponding to room temperature and below. The majority of experiments using acoustic techniques have concentrated on the room-temperature region and yield $z_{r,0}$ values in the 4−6 range, which correspond to $\sigma_r \approx 8-12$ Å$^2$ (not shown). The ultrasonic measurements of Prangsma et al.[49] extending down to 77 K constitute an exception. The agreement between these measurements and our present results is good. The same temperature region was investigated in supersonic jets by Miller and Andres,[17] who used TOF measurements and energy balance in weak expansions from a slit nozzle, where cooling and rarefaction are relatively slow as compared with pinhole nozzles,[4] in order to obtain the rotational relaxation cross section in the 300−80 K energy range; their values are larger than ours. In general, jet experiments sample lower temperatures. Poulsen and Miller[22] used a combination of energy balance and electron beam fluorescence measurements to obtain $\sigma_r$ from relatively weak expansions of nitrogen from a circular nozzle; their estimated value of 14 Å$^2$ (not shown), which should correspond to an approximate temperature of 60 K, is lower than all the rest. As commented on above, Belikov et al.[30,31] have reported rotational relaxation cross sections over wide temperature range from very detailed electron beam fluorescence experiments. Their values agree well with ours down to ≈50 K, but below this temperature, the values of Belikov et al. become gradually larger. Ilyukhin at al.[26] have reported $z_r$ values from CARS measurements between ≈20 and 40 K; from their $z_r$ and from their assumed $\sigma_c(T)$ ($\sigma_c = \sigma_0(1 + C/T)$ with $\sigma_0 = 30.32 \times 10^{-15}$ cm$^{-2}$ and $C$ = 105 K) the rotational relaxation cross sections represented in the figure have been obtained. These values are larger than ours and also somewhat larger than those of Belikov et al.[31]

The results of recent theoretical calculations are also shown. The method of classical trajectories has been used for the derivation of rotational relaxation cross sections and transport coefficients for nitrogen.[51−53] These calculations, performed with realistic intermolecular potentials including ab initio points, are mostly centered on the high-temperature region, but in some cases extend down to 100 K. In the 300−100 K interval, the $\sigma_r$ provided by these calculations grows from 10 to 20 Å$^2$, in good agreement with most of the experimental determinations just commented on. Although the values of $\sigma_r$ given by eq 8 with the parameters estimated by our data are in good agreement with these results, it should be stressed here that our jet experiments are not sensitive in this temperature region. A Monte Carlo simulation of rotational relaxation in jets, extending to much lower temperatures (40 K), has been reported by Cameron and Harland.[50] In this study, however, the collisional processes are modeled in a much simpler way by coupling translation and rotation through an energy dependent parameter accounting for the fraction of inelastic collisions. The actual value of this parameter is determined from diverse literature data corresponding mostly to $T > 100$ K. The $N_2$ rotational relaxation cross sections obtained from their $z_r$ and $\sigma_c$ are in good agreement with the higher temperature measurements of Miller and Anders, but are larger than all of the other determinations shown in this figure. In particular, in the 100−300 K temperature range they are larger than the $\sigma_r$ values from the trajectory calculations just mentioned.[51−53] It should be noted that for $T < 50$ K the $\sigma_r$ compatible with our measurements are lower than the other experimental values[26,31] reported in this temperature range.

The low-temperature rotational relaxation of methane has not been studied so thoroughly, and to the best of our knowledge no experimental relaxation cross sections have been reported for $T < 77$ K. Gallagher and Fenn[18] used TOF measurements and energy balance to determine an effective $z_r$ of 15 referred to a $\sigma_c$ = 45.6 Å$^2$; a much higher $z_r$ would be obtained with a proper low-temperature $\sigma_c$. Their experimental conditions ($T_0$ = 298 K, $p_0d_{eff}$ up to 67 mbar cm) are comparable to those from the present work, and their $z_r$ value is clearly at variance with ours. In the lower panel of Figure 9 we have represented the acoustic results of Prangsma et al.[49] down to 77 K and the Monte Carlo calculations of Cameron and Harland,[50] who used high-temperature acoustic relaxation data for the estimation of their rotation−translation coupling parameter. The agreement between the three sets of data is good. The present results suggest that although the room-temperature cross section for the rotational relaxation of nitrogen is larger than that of methane, the growth of the latter with decreasing temperature is more pronounced. For both substances, the growth of $\sigma_r$ with decreasing $T$ is faster than that of $\sigma_c$, and the number of collisions needed to relax the rotational degree of freedom decreases notably for very low temperatures. This fact could explain the approximate thermal distributions of rotational levels obtained in all the spectra.

In the previous paragraphs we have compared the rotational relaxation cross sections obtained from our data with those from different sources including energy balance, acoustic techniques, and theoretical calculations. In the last part of this discussion we will compare directly our SRS rotational temperatures with measurements from other spectroscopic techniques, allowing also a direct determination of rotational-state distributions. We

restrict our comparison to flows from room-temperature gas sources with Knudsen numbers within the range of our measurements ($p_0 d_{eff} < 150$ mbar cm for $N_2$ and $<200$ mbar cm for $CH_4$). The results of this comparison are illustrated in Figures 5 and 6. An interesting general discussion on internal-state populations in supersonic free jets can be found in ref 36.

In the left panel of Figure 5 we have represented the jet rotational temperatures corresponding to comparatively weak expansions ($p_0 d_{eff} < 10$ mbar cm) of nitrogen. For these conditions, all experimental techniques yield temperatures higher than those of the $\gamma = 1.4$ isentropic curve. For the stronger expansions ($p_0 d_{eff} > 30$ mbar cm) shown in the right panel, the deviations from the isentropic curve and the scatter of the data from different methods are much smaller. The results for $CH_4$ are shown in Figure 6; here again the weakest expansion ($p_0 d_{eff} = 9$ mbar cm) shows a neat deviation and the stronger ones lie all much closer to the isentropic curve.

The electron beam fluorescence technique has been extensively used for the study of supersonic jets of $N_2$ since the pioneering work of Muntz.[27] However, the interpretation of the data from this technique is not immediate, and special care must be paid to the possible influence of secondary electrons on the observed state distributions (see refs 29, 36, 46 and references therein). We have commented above on the rotational relaxation rate constants obtained by Belikov et al.[30,31] using this technique. In Figure 5 we have represented some of the results of Coe et al.[29] for a set of different source conditions. The gradual departure from the isentropic curve with decreasing $p_0 d_{eff}$ is readily appreciable in this figure. The authors did not interpret their relaxation data in terms of a temperature dependent relaxation cross section, but used rather a simple model with a single effective rotational collision number for the whole set of expansions considered ($p_0 d_{eff} = 2.1$ to $p_0 d_{eff} = 135$ mbar cm); their value $z_r = 1.9$ is thus to be interpreted as an estimate of the average rotational collision number for the wide range of terminal conditions corresponding to these experiments.

The REMPI results of Mazely and Smith[32] on the rotational relaxation of $N_2$ show a somewhat larger dispersion than those reported from other techniques, but given the high sensitivity of the experimental method, extend to much larger distances and allow an effective sampling of the transition from continuous to molecular flow. In Figure 5 only results up to $x/d_{eff} = 25$ are shown, but the data reported in ref 32 (corresponding to an expansion with $p_0 d_{eff} = 9$ mbar cm) extend to $x/d_{eff} > 60$. In this experiment the rotational temperature stabilizes at $T_r = 15-20$ K for distances larger than $x/d_{eff} \approx 30$, in good accordance with the predictions of the Boltzmann equation model of ref 10 and also in good agreement with the quitting surface location estimated from the sudden freeze model of eq 4 and with the terminal rotational temperature obtained for our $N_2$ expansion with $p_0 d_{eff} = 7$ mbar cm (see upper panel of Figure 7).

Spectra of $N_2$ in jets have also been recorded by using different Raman techniques. Luijks et al.[24] used spontaneous Raman spectroscopy to measure temperatures in the jet. Their results for $p_0 d_{eff} = 33$ mbar cm are represented in the right panel of Figure 5. These authors derived for their free jets an effective rotational collision number of 1 referred to a constant rigid sphere $\sigma_c$. Re-scaling this value with the low temperature $\sigma_c$ from eq 5 one gets $z_r \approx 2-3$, in accordance with most other results. Huber-Wälchli and Nibler[25] derived rotational temperatures from low-resolution CARS spectra recorded at $x/d_{eff} = 10$ for three weak expansions ($p_0 d_{eff} < 12$ mbar cm); their values (not shown) are in good agreement with those from electron beam fluorescence under similar conditions.[28,29] The temperatures derived from the CARS spectra of Ilyukhin et al.[26] are shown in Figure 5. The rotational relaxation cross sections obtained from these measurements were commented on in the discussion of Figure 9. Finally, Barth et al.[54] have also reported rotational temperatures in a free jet of nitrogen ($p_0 d_{eff} = 40$ mbar cm) from coherent Stokes Raman spectra (CSRS).

As indicated above, there is much less experimental information on the low-temperature rotational relaxation of methane than on that of nitrogen, and the direct determinations of temperature in jets are largely restricted to Raman techniques. In their spontaneous Raman spectra, Luijks et al.[24] found thermal distributions with different $T_r$ for the different spin varieties of $CH_4$; furthermore the 9:5:2, high-temperature theoretical ratio of the F:A:E spin modifications is surprisingly obtained only at large distances from the nozzle exit. The rest of the spectroscopic measurements of $CH_4$ in jets, both from IR[35] and Raman[33,34] techniques, including those from the present work can be well accounted for by assuming a unique $T_r$ and the high-temperature abundance ratios for the different spin varieties as indicated in section 2. The CARS spectra of Huisken and Pertsch[33] yield temperatures colder than those of the $\gamma = 1.33$ isentrope. As a possible explanation for this anomalous behavior, the authors suggest an insufficient opening of the plunger in their pulsed valve that could lead to the formation of a small channel causing a precooling of the gas before the nozzle exit. An alternative explanation based also on an incomplete opening would be the assumption of an effective nozzle diameter smaller than the nominal one by ≈30%.

## 5. Conclusions

The combination of molecular spectroscopy and time-of-flight measurements is a useful tool for the global description of supersonic expansions. In particular the high-resolution SRS technique used in the present work allows the determination of rotational state distributions of small molecules. For the two species investigated ($N_2$ and $CH_4$) the measured spectra can be always simulated within experimental error by assuming thermal distributions of rotational states.

To a good approximation very simple treatments such as the sudden freeze model or a linear relaxation equation for the coupling of rotation and translation can provide a satisfactory description of free jets from moderately weak ($p_0 d_{eff} \approx 7-9$ mbar cm), to relatively strong ($p_0 d_{eff} \approx 60-140$ mbar cm) expansions. For weaker expansions the present SRS technique is not sensitive enough and the isentropic behavior of translation might not be quite justified. For stronger expansions, aggregation processes may begin for the gases under study. Although the "sudden freeze" model represents a too extreme physical approximation, it is not entirely unreasonable for the description of translation in the jet since the efficiency of momentum transfer is so high that it continues virtually until the "last" collision. Both a rigid sphere cross section and a cross section based on the attractive part of a Lennard-Jones potential can describe well the degree of translational cooling attained in supersonic expansions of the $N_2$ and $CH_4$ from room-temperature sources. The assumption of a linear relaxation equation for the coupling of rotation and translation can account approximately both for the near isentropic temperatures obtained in the stronger expansions and for the deviations of the isentropic behavior observed in the weaker ones.

The low-temperature cross sections for rotational relaxation obtained from the present measurements are noticeably larger than those at room temperature, in agreement with most experimental and theoretical estimates. In fact, with decreasing temperature, the relaxation cross sections grow faster than the collision cross sections (usually assumed to be proportional to

$T^{-1/3}$). As a consequence, the number of collisions needed to relax the rotational degree of freedom becomes smaller with decreasing temperature. Whereas the room-temperature rotational collision numbers are 4−6 for $N_2$ and 12−14 for $CH_4$, for temperatures between 15 and 50 K, the rotational collision numbers for both molecules are in the 2−4 range.

**Acknowledgment.** The technical advice and support of J. M. Castillo, M. A. Moreno, and J. Rodríguez have been most valuable for the achievement of the present experiments. We are indebted to T. Díez Rojo for her help with the evaluation of the data and to F. J. Aoiz and V. Sáez Rábanos for their careful reading of the manuscript. This work has been funded by the DGICYT of Spain under Grants PB94-0108 and PB95-09178-03.

## References and Notes

(1) Scoles, G., Ed. *Atomic and Molecular Beam Methods*; Oxford University Press: New York, 1988 (vol. 1), 1992 (vol. 2).
(2) Anderson, J. B. In *Molecular Beams and Low-Density Gas Dynamics*; Wegener, P. P., Ed.; Dekker: New York, 1974.
(3) Campargue, R. *J. Phys. Chem.* **1984**, *88*, 4466.
(4) Miller, D. R. In *Atomic and Molecular Beam Methods (vol. 1)*; Scoles, G., Ed.; Oxford University Press: New York, 1988.
(5) Hirschfelder, J. O.; Curtiss, C. F.; Bird, R. *Molecular Theory of Gases and Liquids*; J. Wiley & Sons: New York, 1954.
(6) Lambert, J. D. *Vibrational and Rotational Relaxation in Gases*; Oxford University Press: Oxford, 1977.
(7) Pirumov, U. G.; Roslyakov, G. S. *Gas Flow in Nozzles*; Springer-Verlag: Berlin, Heidelberg, 1986.
(8) Tejeda, G.; Maté, B.; Fernández Sánchez, J. M.; Montero, S. *Phys. Rev. Lett.* **1996**, *76*, 34.
(9) Toennies, J. P.; Winkelmann, K. *J. Chem. Phys.* **1977**, *66*, 3965.
(10) Randeniya, L. K.; Smith, M. A. *J. Chem. Phys.* **1990**, *93*, 661.
(11) Beijerinck, H.; Verster, N. *Physica* **1981**, *111C*, 327.
(12) Klots, C. E. *J. Chem. Phys.* **1980**, *72*, 192.
(13) Cameron, B. R.; Harland, P. W. *J. Chem. Soc., Faraday Trans.* **1993**, *89*, 1903.
(14) Anderson, J. B.; Fenn, J. B. *Phys. Fluids* **1965**, *8*, 780.
(15) Sharma, P. K.; Young, W. S.; Rodgers, W. E.; Knuth, E. L. *J. Chem. Phys.* **1975**, *62*, 341.
(16) Quah, G. C.; Fenn, J. B.; Miller, D. R. *Rarefied Gas Dynamics, 11th Int. Symposium*; Campargue, R., Ed.; Comissariat a l'Energie Atomique: Paris 1979; p 855.
(17) Miller, D. R.; Andres, R. P. *J. Chem. Phys.* **1967**, *46*, 3418.
(18) Gallagher, R. J.; Fenn, J. B. *J. Chem. Phys.* **1974**, *60*, 3487.
(19) Quah, C. G. *Chem. Phys. Lett.* **1979**, *63*, 141.
(20) Coe, D.; Robben, F.; Talbot, L.; Cattolica, R. *Phys. Fluids* **1980**, *23*, 715.
(21) Brusdeylins, G.; Meyer, H. D. *Rarefied Gas Dynamics, 11th Int. Symposium*; Campargue, R. Ed.; Comissariat a l'Energie Atomique: Paris 1979; p 919.
(22) Poulsen, P.; Miller, D. R. *Rarefied Gas Dynamics, 10th Int. Symposium*; Potter, J. L., Ed.; Progress in Astronautics and Aeronautics; AIAA: New York, 1974; Vol. 51, p 899.
(23) Yamazaki, S.; Taki, M.; Fujitani, Y. *J. Chem. Phys.* **1981**, *74*, 4476.
(24) Luijks, G.; Stolte, S.; Reuss, J. *Chem. Phys.* **1981**, *62*, 217.
(25) Huber-Wälchli, P.; Nibler, J. W. *J. Chem. Phys.* **1982**, *76*, 273.
(26) Ilyukhin, A. A.; Pykhov, R. L.; Smirnov, V. V.; Marowski, G. *Appl. Phys. B* **1990**, *51*, 1992.
(27) Muntz, E. P. *Phys. Fluids* **1962**, *5*, 80.
(28) Marrone, P. V. *Phys. Fluids* **1967**, *10*, 521.
(29) Coe, D.; Robben, F.; Talbot, L.; Cattolica, R. *Phys. Fluids* **1980**, *23*, 706.
(30) Belikov, A. E.; Sukhinin, G. I.; Sharafutdinov, R. G. *Rarefied Gas Dynamics, 16th Symposium*; Muntz, E. P., Weaver, D. P., Campbell, D. H., Eds.; Progress in Astronautics and Aeronautics; AIAA Inc.: Washington, 1989; Vol. 117, p 50.
(31) Belikov, A. E.; Sharafutdinov, R. G.; Strekalov, M. L. *Chem. Phys. Lett.* **1994**, *231*, 1994.
(32) Mazely, T. L.; Smith, M. A. *J. Phys. Chem.* **1990**, *94*, 6930.
(33) Huisken, F.; Pertsch, T. *Appl. Phys. B* **1986**, *41*, 173.
(34) Valentini, J. J.; Esherick, P.; Owyoung, A. *Chem. Phys. Lett.* **1980**, *75*, 1980.
(35) Amrein, A.; Quack, M.; Schmitt, U. *J. Phys. Chem.* **1988**, *92*, 5455.
(36) Campargue, R.; Gaveau, M. A.; Lebéhot, A. *Rarefied Gas Dynamics, 14th Symposium*; Oguchi, H., Ed.; University of Tokyo Press: Tokyo 1984; Vol. II, p 551.
(37) Abad, L.; Bermejo, D.; Herrero, V. J.; Santos, J.; Tanarro, I. *Rev. Sci. Instrum.* **1995**, *66*, 3826.
(38) Bermejo, D.; Santos, J.; Cancio, P.; Domenech, J. L.; Domingo, C.; Orza, J. M.; Ortigoso, J.; Escribano, R. *J. Raman Spectrosc.* **1990**, *21*, 197.
(39) Santos, J.; Cancio, P.; Domenech, J. L.; Rodriguez, J.; Bermejo, D. *Laser Chem.* **1992**, *12*, 53.
(40) Haberland, H.; Buck, U.; Tolle, M. *Rev. Sci. Instrum.* **1985**, *56*, 1712.
(41) Auerbach, D. J. In *Atomic and Molecular Beam Methods (vol. 1)*; Scoles, G., Ed.; Oxford University Press: New York, 1988.
(42) Abad, L. Ph.D. Thesis, Universidad Complutense, Madrid, 1996.
(43) Ashkenas, H.; Sherman, F. H. *Rarefied Gas Dynamics, 4th Symposium*; De Leeuw, J., Ed.; Academic Press: New York, 1966; Vol. 2, p 84.
(44) Santos, J.; Abad, L.; Bermejo, D.; Herrero, V. J.; Tanarro, I. To be published.
(45) Rabitz, H.; Lam, S. H. *J. Chem. Phys.* **1975**, *63*, 3532.
(46) Belikov, A. E.; Burshtein, A. I.; Doglgushev, S. V.; Storozhev, A. V.; Strekalov, M. L.; Shukhinin, G. I.; Sharafutdinov, R. G. *Chem. Phys.* **1989**, *139*, 239.
(47) Liu, S.; Zhang, Q.; Chen, C.; Zhang, Z.; Dai, J.; Ma, X. *J. Chem. Phys.* **1995**, *102*, 3617.
(48) Mazely, T. L.; Roehrig, G. H.; Smith, M. A. *J. Chem. Phys.* **1995**, *103*, 8638.
(49) Prangsma, G. J.; Alberga, A. H.; Beenakker, J. J. M. *Physica* **1973**, *64*, 278.
(50) Cameron, B. R.; Harland, P. W. *J. Chem. Soc., Faraday Trans.* **1989**, *89*, 3517.
(51) Nyeland, C.; Poulsen, L. L.; Billing, G. D. *J. Phys. Chem.* **1984**, *88*, 1216.
(52) Nyeland, C.; Billing, G. D. *J. Phys. Chem.* **1988**, *92*, 1752.
(53) Billing, G. D.; Wang, L. *J. Phys. Chem.* **1992**, *96*, 2672.
(54) Barth, H.-D.; Huisken, F.; Ilyukhin, A. A. *Appl. Phys. B* **1991**, *52*, 84.